Broadband Electrical Sensing of Nucleus Size in a Live Cell from 900 Hz to 40 GHz

Xiaotian Du
Department of Electrical and
Computer Engineering
Lehigh University
Bethlehem, PA, USA
xid415@lehigh.edu

Caroline Ladegard
Department of Bioengineering
Lehigh University
Bethlehem, PA, USA
cal618@lehigh.edu

Xiao Ma
Department of Electrical and
Computer Engineering
Lehigh University
Bethlehem, PA, USA
xim214@lehigh.edu

Xuanhong Cheng Department of Bioengineering, Lehigh University Bethlehem, PA, USA xuc207@lehigh.edu

James C. M. Hwang
Department of Materials Science
and Engineering
Cornell University
Ithaca, NY, USA
jch263@cornell.edu

Abstract—Live Jurkat cells were trapped by dielectrophoresis on a coplanar waveguide and the resulted changes in its reflection and transmission coefficients were measured from 900 Hz to 40 GHz. The measurement confirms that the decrease of nucleus size in a cell increases its impacts on both the reflection and transmission coefficients. Being fast, compact and label free, broadband electrical sensing may be used to detect other changes of the nucleus morphology and DNA content, which could be useful for cancer diagnosis.

Keywords—Biological cells, biosensors, nuclear measurements, microwave measurements, ultra wideband technology

I. INTRODUCTION

Sensing the nucleus morphometry and DNA content in a biological cell is critical to identification of cancer cells, because the change in the cell nucleus can reflect gene mutation, altered gene expression, and tumor development [1]. To this end, optical microscopy and flow cytometry have been developed, but usually require cell labeling and terminal testing [2]. By contrast, microwave sensing of individual biological cells [3], [4], especially over an ultrawide bandwidth of 9 kHz to 9 GHz [5], has been used as a label-free and noninvasive technique to sense the nucleus size in a live cell [6]. This work expands on [6] by extending further the bandwidth to 900 Hz–40 GHz, especially to capture the peak change around 20 GHz in the reflection coefficient of a coplanar waveguide (CPW) with a live cell trapped on it.

II. EXPERIMENTS

Fig. 1 shows that the experimental setup is similar to that of [6] except in the microfluidic channel design. The setup is based mainly on a homemade microwave probe station and a Nikon Eclipse Ti-E inverted fluorescence microscope. The microscope

is equipped with a high-speed (100 frame/s) three-color Hamamatsu video camera for simultaneous optical and electrical measurements in real time. The device under test (DUT) comprises a gold CPW, 1-cm long and 0.5- μ m thick, which is sandwiched between a 0.5-mm-thick quartz substrate and a 5-mm-thick polydimethylsiloxane (PDMS) cover. The bottom side of the PDMS cover is molded with a microfluidic channel, which intersects the CPW at a right angle as shown in Fig. 2(a). The gap between the center and ground electrodes of the CPW is 16 μ m. The center electrode is mostly 200- μ m-wide except under the microfluidic channel, where it is tapered down to a 10 μ m by 10 μ m gap. This gap is used to trap a live cell by applying a dielectrophoresis (DEP) signal to the CPW.

Fig. 2(b) shows that the microfluidic channel has been redesigned to add sheath flows to help focus the center flow.

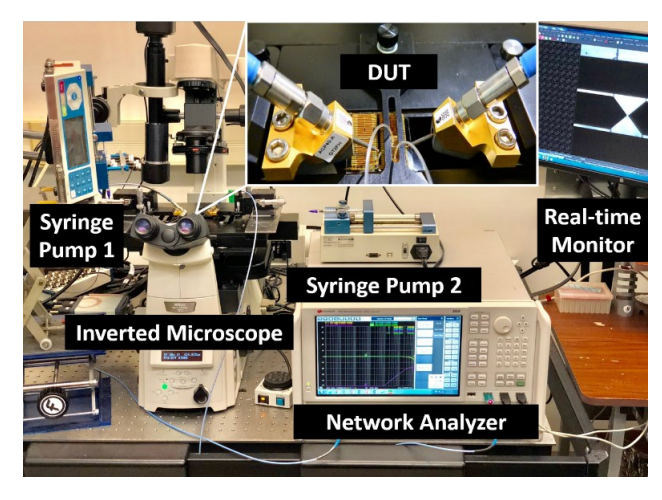


Fig. 1. Experimental setup for sensing the nucleus size of a live cell using a homemade microwave probe station on an inverted fluorescence microscope.

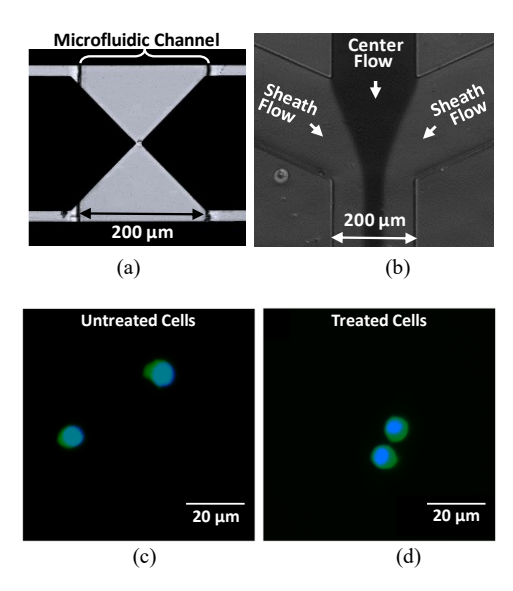


Fig. 2. Bright-field micrographs of (a) a live Jurkat cell trapped on a CPW by DEP and (b) a microfluidic junction with the center flow purposely dyed darker. Fluorescence micrographs of (c) untreated and (d) treated cells stained blue (with Hoeschst 33342) and green (with Calcein-AM) to reveal their nucleus and cytoplasm sizes, respectively.

While the center flow contains cells suspended in a sucrose solution, the sheath flows contain only the sucrose solution. Although the microfluidic channel remains 100- μ m-thick and 200- μ m-wide, by controlling the center and total sheath flow rates at 0.25 $\mu\ell/min$ and 0.75 $\mu\ell/min$, respectively, the center flow is narrowed down to approximately 40- μ m-wide. This increases the DEP trap rate from approximately one cell per min to one cell every 10 s.

A Keysight Technologies N5247B PNA-X network analyzer was used to apply the DEP signal to the CPW via a pair of Cascade Microtech ACP40 GSG probes. After validating the crossover frequencies over which the Clausius-Mossotti function changes sign [8], a 3-dBm signal is used to trap the cell at 5 MHz and to detrap it at 10 kHz. Once a cell is trapped, the same network analyzer is used to generate a 15-dBm signal for measuring the scattering (S) parameters of the CPW between 900 Hz and 40 GHz. Afterward, the cell is detrapped and the S parameters quickly remeasured to establish the background level. The difference between the two sets of consecutively measured S parameters reflects the presence of the cell. Thus, the change in the magnitude of the reflection coefficient S₁₁ is defined as:

$$\Delta |S_{11}| = 10 \cdot \log |S_{11}(w/\text{cell})/S_{11}(w/\text{ocell})|$$

$$= 10 \cdot \log |S_{11}(w/\text{cell})| - 10 \cdot \log |S_{11}(w/\text{ocell})|.$$
(1)

Similarly, the change in the magnitude of the transmission coefficient S_{21} is defined as:

$$\Delta |S_{21}| = 10 \cdot \log |S_{21}(w/\text{cell})/S_{21}(w/\text{ocell})|
= 10 \cdot \log |S_{21}(w/\text{cell})| - 10 \cdot \log |S_{21}(w/\text{ocell})| .$$
(2)

For proof of concept, Jurkat human lymphocyte cells are chosen for their large size, simple structure, and nonadherent

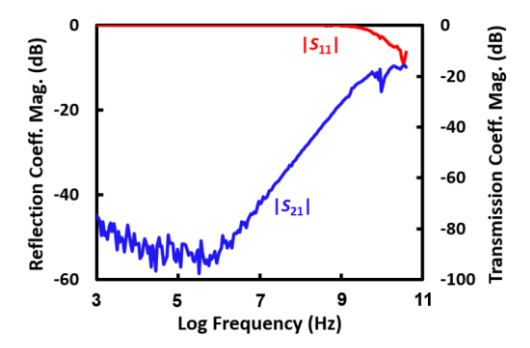


Fig. 3. Measured magnitudes of reflection coefficient $|S_{11}|$ and transmission coefficient $|S_{21}|$ of the CPW without any cell trapped.

nature. To shrink the nucleus size, half of the cells were treated in a solution of 460 µg/mℓ staurosporine in dimethyl sulfoxide for 1 h [7]. The other half of untreated cells were kept as a control. Fluorescent microscopy (Fig. 2) confirms that with the treatment, the average nucleus-to-cytoplasm diameter ratio decreases from 77% to 71% [6]. All cells, treated or not, were twice washed and re-suspended in an isotonic solution of 8.5% sucrose and 0.3% dextrose to a concentration of 3×10^6 cell/mℓ before electrical sensing. Cell viability was verified in a separate experiment with Trypan Blue dye, which showed more than half of cells survived after 10 h [4].

III. RESULTS AND DISCUSSION

Fig. 3 shows measured $|S_{11}|$ and $|S_{21}|$ of the CPW without any cell trapped. It can be seen that $|S_{11}|$ and $|S_{21}|$ are well behaved in general, except resonances around 10 GHz where the length of the CPW is approximately half of the wavelength. Additionally, below 10 MHz, $|S_{21}|$ becomes rather noisy where it approaches the noise floor.

Using seven treated cells and seven untreated cells, fourteen single-cell measurements were made. With a cell trapped, changes in $|S_{11}|$ and $|S_{21}|$ are so small (0.1 dB or less) that they are not discernable on the scale of Fig. 3. The changes can be seen only when plotted by themselves as shown in Fig. 4. Each curve in Fig. 4 represents the average of seven measurements made on seven cells with the standard deviation indicated. It can be seen that similar to [6], the change in $|S_{21}|$ is broader and more prominent, whereas the change in $|S_{11}|$ is weaker but peaks at high frequencies. However, different from [6], the peaks are well captured in the present measurement. As the result, it can be clearly seen that for a treated cell, the peak change in $|S_{11}|$ shifts from around 20 GHz to around 8 GHz. Depending on the experimental design, it may be easier to sense the frequency shift in the $|S_{21}|$ change or the magnitude increase in the $|S_{21}|$ change.

According to sensitivity analysis [9], signals above f_0 can readily bypass the cell membrane, where

$$f_0 \approx 1 / \left(2\pi C_C \sqrt{R_C Z_0} \right), \tag{3}$$

 C_C is the cytoplasm capacitance, R_C is the cytoplasm resistance, and Z_0 is the system impedance. For an untreated Jurkat cell, C_C = 6.4 fF and R_C = 1.2 M Ω . With Z_0 = 50 Ω , $f_0 \approx$ 3 GHz. In this case, the changes in $|S_{11}|$ and $|S_{21}|$ mainly reflect the change in C_C . Specifically,

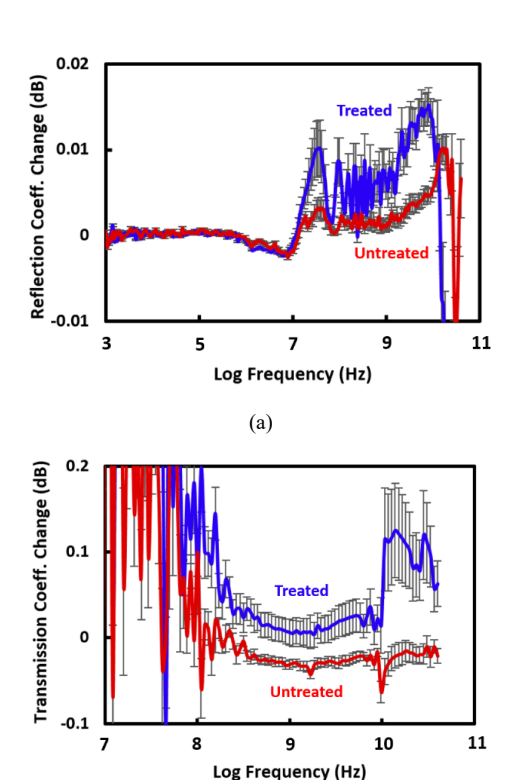


Fig. 4. Measured changes in $|S_{11}|$ and $|S_{21}|$ of the CPW with a staurosporine-treated or an untreated cell trapped.

$$\Delta |S_{11}|/|S_{11}| \approx -(2\omega C_C Z_0)^2 (\Delta C_C / C_C)$$
, (4)

and

$$\Delta |S_{21}|/|S_{21}| \approx \Delta C_C/C_C, \qquad (5)$$

where ω is the angular frequency. Note that even at 40 GHz, $2\omega C_C Z_0 \ll 1$, which explains why the $|S_{11}|$ change is much weaker than the $|S_{21}|$ change. For an untreated cell above 3 GHz, the measured changes are positive and negative in $|S_{11}|$ and $|S_{21}|$, respectively. This is consistent with (4) and (5) with a negative ΔC_C , which is, in turn, consistent with a lower dielectric constant for the cytoplasm than that of the sucrose solution ($\varepsilon_C < \varepsilon_S$) [10]– [12]. However, since [9] does not include the dispersion in the dielectric properties of either the cell or the sucrose solution, presently it cannot explain why the $|S_{11}|$ change peaks around 20 GHz. It is possible that while $|S_{21}|$ is sensitive to the primary resonance around 10 GHz independent of the cell, $|S_{11}|$ is sensitive to the second-harmonic resonance around 20 GHz, which is dependent on the reflection from the cell, treated or not. The above observation indicates that, to expand the bandwidth above 9 GHz, it is important to not only consider the dielectric dispersion, but also to reduce the CPW length.

Further, the analysis of [9] is based on a single-shell cell model [13], so that C_C actually includes contributions from both the cytoplasm and the nucleus. In general, $\varepsilon_C < \varepsilon_S < \varepsilon_N$ for a human lymphocyte cell, where ε_N is the dielectric constant of the nucleus [14]. For a treated cell with a smaller nucleus, the volume ratio of the cytoplasm to nucleus increases and the effect of ε_C on ΔC_C increases, making C_C even smaller than that of an

untreated cell. This can explain why the $|S_{11}|$ change is even more positive for a treated cell than for an untreated cell. However, a smaller C_C should cause the $|S_{21}|$ change for a treated cell to be less negative but not to become positive. This dilemma awaits more careful quantitative analysis based on a double-shell model [15].

IV. CONCLUSION

Live Jurkat cells were trapped by dielectrophoresis on a CPW and the resulted changes in its reflection and transmission coefficients were measured from 900 Hz to 40 GHz. By comparing chemically treated cells with those untreated, experimentally it was found that the decrease of nucleus size in a cell generally increases its impacts on both the reflection and transmission coefficients. This increase is consistent with a decrease in the cytoplasm capacitance, which, according to the single-shell model, includes contributions from both the cytoplasm and the nucleus. However, before the present technique can be used as a fast, compact and label-free technique to sense other changes in the nucleus morphology and DNA content, more careful quantitative analysis based on a double-shell cell model with dispersive permittivities is needed.

ACKNOWLEDGMENT

This work was supported in part by the U.S. National Science Foundation under Grant ECCS-1809623, Army Research Office under Grant W911NF-14-1-0665, and Air Force Office of Scientific Research under Grant FA9550-16-1-0475.

REFERENCES

- [1] T. Misteli, "Beyond the sequence: Cellular organization of genome function," *Cell* vol. 128, no. 4, pp. 787–800, Feb. 2007.
- [2] M. A. Al-Abbadi, "Basics of cytology," Avicenna J. Med., vol. 1, no. 1, pp. 18–28, Jul.-Sep. 2011.
- [3] K. Grenier, D. Dubuc, T. Chen, F. Artis, T. Chretiennot, M. Poupot, and J.-J. Fournie, "Recent advances in microwave-based dielectric spectroscopy at the cellular level for cancer investigations," *IEEE Trans. Microw. Theory Techn.*, vol. 61, no. 5, pp. 2023–2030, May 2013.
- [4] Y. Ning, C. Multari, X. Luo, C. Palego, X. Cheng, J. C. M. Hwang, A. Denzi, C. Merla, F. Apollonio, and M. Liberti, "Broadband electrical detection of individual biological cells," *IEEE Trans. Microw. Theory Techn.*, vol. 62, no. 9, pp. 1905–1911, Sep. 2014.
- [5] X. Ma, X. Du, H. Li, X. Cheng, and J. C. M. Hwang, "Ultra-wideband impedance spectroscopy of a live biological cell," *IEEE Trans. Microw. Theory Techn.*, vol. 66, no. 8, pp. 3690–3696, Aug. 2018.
- [6] X. Du, C. Ladegard, X. Ma, X. Cheng and J. C. M. Hwang, "Ultrawideband electrical sensing of nucleus size in a live cell," in *European Microwave Conf. (EuMC)*, Paris, France, Oct. 2019, pp. 208–211.
- [7] I. Chowdhury, W. Xu, J. K. Stiles, A. Zeleznik, X. Yao, R. Matthews, K. Thomas, and W. E. Thompson, "Apoptosis of rat granulosa cells after staurosporine and serum withdrawal is suppressed by adenovirus-directed overexpression of prohibition," *Endocrinology*, vol. 148, no. 1, pp. 206–217, Jan. 2007.
- [8] X. Du, X. Ma, L. Li, H. Li, X. Cheng, J. C. M. Hwang, "Validation of Clausius-Mossotti function in wideband single-cell dielectrophoresis," *IEEE J. Electromagn. RF Microw. Med. Bio.* vol. 3, no. 2, pp. 127–133, Jun. 2019.
- [9] X. Ma, X. Du, L. Li, H. Li, X. Cheng and J. C. M. Hwang, "Sensitivity Analysis for Ultra-Wideband 2-Port Impedance Spectroscopy of a Live Cell," in *IEEE Journal of Electromagnetics, RF and Microwaves in Medicine and Biology*, vol. 4, no. 1, pp. 37-44, March 2020.
- [10] A. Denzi, C. Merla, C. Palego, A. Paffi, Y. Ning, C. R. Multari, X. Cheng, F. Apollonio, J. C. M. Hwang, and M. Liberti, "Assessment of cytoplasm

- conductivity by nanosecond pulsed electric fields," *IEEE Trans. Biomed. Eng.*, vol. 62, no. 6, pp. 1595–1603, Jun. 2015.
- [11] H. Li, A. Denzi, X. Ma, X. Du, Y. Ning, X. Cheng, F. Apollonio, M. Liberti, and J. C. M. Hwang, "Distributed effect in high-frequency electroporation of biological cells," *IEEE Trans. Microw. Theory Techn.*, vol. 65, no. 9, pp. 3503–3511, Sep. 2017.
- [12] X. Jin, M. Farina, X. Wang, G. Fabi, X. Cheng, and J. C. M. Hwang, "Quantitative scanning microwave microscopy of the evolution of a live biological cell in a physiological buffer," *IEEE Trans. Microw. Theory Techn.*, vol. 67, no. 12, pp. 5438–5445, Dec. 2019.
- [13] T. Hanai, K. Asami, and N. Koizumi, "Dielectric theory of concentrated suspension of shell," *Bull. Inst. Chem. Res.*, Kyoto University, vol. 57, pp. 297–305, Oct. 1979.
- [14] I. Ermolina, Y. Polevaya, Y. Feldman, B.-Z. Ginzburg, and M. Schlesinger, "Study of normal and malignant white blood cells by time domain dielectric spectroscopy," *IEEE Trans. Dielectr. Electr. Insul.*, vol. 8, no. 2, pp. 253–261, Apr. 2001.
- [15] K. Asami, Y. Takahashi and S. Tabshima, "Dielectric properties of mouse lymphocytes and erythrocytes," *Biochim. Biophys. Acta*, vol. 1010, no. 1, pp. 49–55, Jan. 1989.